J|A|C|S
ARTICLES
Published on Web 06/05/2007

Surface Effects on Quantum Dot-Based Energy Transfer

Smita Dayal and Clemens Burda*

Contribution from the Center for Chemical Dynamics and Nanomaterials Research, Department of Chemistry, Case Western Reserve University, Cleveland, Ohio 44106

Received March 1, 2007; E-mail: burda@case.edu

Abstract: CdSe quantum dot (QD)−phthalocyanine (Pc) conjugates were prepared as energy transfer donor−acceptor pairs, and the efficiency of the energy transfer process in this system was investigated as a function of QD size and under different surface chemistry conditions. The kinetics and efficiency of the energy transfer process were studied by femtosecond time-resolved laser spectroscopy. We observed that the energy transfer efficiency does not follow a linear dependence on spectral overlap integrals as predicted by the Förster theory for molecules. This observation is found to be due to the involvement of QD surface states in the energy transfer process from the photoexcited QDs to the molecular energy acceptor.

Introduction

This study aims to elucidate the underlying factors of the energy transfer (ET) process at the quantum dot (QD)−molecule interface using steady-state and femtosecond time-resolved laser spectroscopy. Photoluminescent QDs are often used as sensitizers in imaging analysis and for an increasing range of applications in biomedicine.[1] Such research often deals with energy transfer (ET) from QDs to molecules in photodynamic therapy,[2] imaging,[3] and drug delivery.[4] Förster Resonance Energy Transfer (FRET) was used as a probe for single mismatches in DNA hybridization[5] and dynamics of DNA replication and telomerization,[6] as well as to study inhibition assays based on the modulation of FRET efficiencies.[7] FRET from QDs to molecular probes was also developed for nanoscale sensors for TNT,[8] maltose,[9] protease,[10] and enzymatic activity.[11] In general, QDs show good photoluminescence quantum yields, excellent photostability, narrow emission, and broad excitation spectra, which are needed for efficient sensitization. In most cases, the ET in QD conjugates is discussed as a pure FRET process. The Förster theory in ET predicts a negative sixth root dependence of the ET efficiency on the D−A separation distance and requires a linear proportionality of the ET efficiency on the overlap integral.[12] However, recent reports show evidence for a zeroth to negative-fourth power dependence on distance, depending on the nature of the constituents.[13] It was demonstrated that in short-range ET, from QDs to molecular energy acceptors, other parameters appear to play a role in addition to the Förster mechanism.[14] Such non-Förster type parameters for QD conjugates involve among others the effects of surface variations, degree of interdigitization, and contributions of surface states. Recently, the dependence of the ET efficiency on the donor−acceptor linker chain length was investigated[14] in CdSe QD−phthalocyanine conjugates (QD−Pc) and it was found that the ET efficiency increased with improved interdigitization of the Pc linker chain with the organic QD capping layer, which resulted in a better coupling of the acceptor to the donor QD moiety. In a complex system which includes QDs, additional surface or capping related factors can therefore play a significant role. To date the role of surface states in QD-based ET was so far not taken explicitly into account in studying the mediation of QD-based ET. Here, we show that the issue of surface state mediation in the ET process can be investigated by synthesizing a homologous series of QD-based donor−acceptor (DA) pairs with a systematic change in overlap integral and studying the

(1) (a) Alivisatos, A. P. *Science* **1996**, *271*, 933. (b) Chan, W. C.-W.; Nie, S. *Science* **1998**, *281*, 2016. (c) Han, M.; Gao, X.; Su, J. Z.; Nie, S. *Nat. Biotechnol.* **2001**, *19*, 631. (d) Klarreich, E. *Nature* **2001**, *413*, 450. (e) Mitchell, P. *Nat. Biotechnol.* **2001**, *19*, 1013. (f) Wu, X.; Liu, H.; Liu, J.; Haley, K. N.; Treadway, J. A.; Larson, J. P.; Ge, N.; Peale, F.; Bruchez, M. P. *Nat. Biotechnol.* **2003**, *21*, 41. (g) Alivisatos, P. *Nat. Biotechnol.* **2004**, *22*, 47.
(2) (a) Samia, A. C. S.; Chen, X.; Burda, C. *J. Am. Chem. Soc.* **2003**, *125*, 15736. (b) Bakalova, R.; Ohba, Z.; Zhelev, Z.; Ishikawa, M.; Baba, Y. *Nat. Biotechnol.* **2004**, *22*, 1360. (c) Bakalova, R.; Ohba, Z.; Zhelev, Z.; Nagase, T.; Jose, R.; Ishikawa, M.; Baba, Y. *Nano Lett.* **2004**, *4*, 1567.
(3) (a) Bruchez, M., Jr.; Moronne, M.; Gin, P.; Weiss, S.; Alivisatos, A. P. *Science* **1998**, *281*, 2013. (b) Jaiswal, J. K.; Mattoussi, H.; Mauro, J. M.; Simon, S. M. **2003**, *21*, 47. (c) Gao, X.; Cui, Y.; Levenson, R. M.; Chung, L.W. K.; Nie, S. *Nat. Biotechnol.* **2004**, *22*, 969.
(4) Roy, I.; Ohulchanskyy, T. Y.; Pudavar, H. E.; Bergey, E. J.; Oseroff, A. R.; Morgan, T.; Dougherty, T. J.; Prasad, P. N. *J. Am. Chem. Soc.* **2003**, *125*, 7860.
(5) Dubertret, M.; Calame, M.; Libchaber, A. J. *Nat. Biotechnol.* **2001**, *19*, 365−370.
(6) Patolsky, F.; Gill, R.; Weizmann, Y.; Mokari, T.; Banin, U.; Willner, I. *J. Am. Chem. Soc.* **2003**, *125*, 13918−13919.
(7) Oh, E.; Hong, Mi-Young.; Lee, D.; Nam Sung-Hun, Yoon, H. C.; Kim, Hak-Sung *J. Am. Chem. Soc.* **2005**, *127*, 3270−3271.
(8) Goldman, E. R.; Medintz, I. L.; Whitley, J. L.; Hayhurst, A.; Clapp, A. R.; Uyeda, H. T.; Deschamps, J. R.; Lassman, M. E.; Mattousi, H. *J. Am. Chem. Soc.* **2005**, *127*, 6744−6751.
(9) Medintz, I. L.; Clapp, A. R.; Mattousi, H. J.; Goldman, E. R.; Fisher, B.; Mauro, J. M. *Nat. Mater.* **2003**, *2*, 630−638.
(10) Shi, L.; Paoli, V. D.; Rosenzweig, N.; Rosenzweig, Z. *J. Am. Chem. Soc.* **2006**, *128*, 10378−10379.
(11) Shi, L.; Rosenzweig, N.; Rosenzweig, Z. *Anal. Chem.* **2007**, *79*, 208−214.
(12) (a) Haugland, R. P.; Yguerabide, J.; Stryer, L. *Proc. Natl. Acad. Sci. U.S.A.* **1969**, *63*, 23. (b) Stryer, L. *Annu. Rev.* **1978**, *47*, 819. (c) Clapp, A. R.; Medintz, I. L.; Mauro, J. M.; Fisher, B. R.; Bawendi, M. G.; Mattoussi, H. *J. Am. Chem. Soc.* **2004**, *126*, 301.
(13) Singh, H.; Bagchi, B. *Curr. Sci.* **2005**, *89*, 1710.
(14) Dayal, S.; Lou, Y. B.; Samia, A. C. S.; Berlin, J.; Kenney, M. E.; Burda, C. *J. Am. Chem. Soc.* **2006**, *128*, 13974.

efficiency and dynamics of the photoinduced ET. Since smaller QDs are known to have more surface trap states compared to the larger dots, due to a higher surface to volume ratio and surface tension, a comparative analysis of the ET dynamics and dependence of the ET efficiency on the spectral overlap integral provides a way to investigate the role of intermediate QD surface states in ET. The spectral overlap between QD emission and Pc absorption depends on the QD size due to quantum confinement effects. Therefore, the validity of the linear spectral overlap dependence of the ET efficiency can be studied. In addition, the involvement of QD surface states can be investigated by modifying the QD surface with organic (TOPO) and inorganic (ZnS) surface layers. The observed results indicate the importance of QD surface passivation, and it becomes evident that QD-based ET cannot be explained based on pure molecular theories alone but that surface states play an additional important role.

CdSe QDs of different sizes were synthesized according to a previously reported method.[15] The molecular energy acceptor Pc 4 was prepared by Kenney et al.[16] and provided in high purity. The synthesized conjugates[14,17] were studied by steady-state absorption and emission as well as femtosecond time-resolved laser spectroscopy. The spectral overlap integral J is tuned by adjusting the size of QDs, and hence varying the emission maximum while keeping the phthalocyanine (Pc) absorption and donor−acceptor (DA) distance constant. On the other hand, to study the influence of inorganic surface passivation of QDs on the ET dynamics, CdSe−ZnS core−shell QDs were synthesized and the ET efficiency was compared to the one of uncapped CdSe QDs. The ET efficiency was evaluated from steady-state emission measurements and by the measured lifetimes of the photoexcited donor in the presence and absence of the acceptor molecule.

Experimental Section

Synthesis and Characterization. CdSe QDs were synthesized following the method of Peng et al.[15] The synthesis was performed using standard airless techniques, and all solvents used were anhydrous. QDs were grown at 250 °C. Samples of various sizes were taken at different reaction times, and the growth of QDs was quenched by injecting samples in cold anhydrous toluene.

On the other hand, core−shell CdSe−ZnS QDs were synthesized by growing a layer of ZnS on as-prepared CdSe dots. Diethyl zinc and hexamethyl disilthiane in TOP were used as the precursors for Zn and S, respectively. Dropwise injection of the capping reagents was carried out at 220 °C over 40 min. The synthesized particles were annealed for an additional 30 min at 220 °C. The resulting ZnS-capped QD sample showed a 5× higher fluorescence quantum yield compared to the uncapped QDs. Prior to the formation of the QD−Pc conjugates, the synthesized QD samples were washed twice by precipitating with anhydrous methanol (Aldrich) and redissolved in anhydrous toluene. For conjugate preparation, Pc 4 was dissolved in anhydrous toluene and mixed with the QD solutions. 8×10^{-6} M Pc and the 5×10^{-6} M QD concentrations were used in all experiments to obtain the maximum energy transfer while still keeping the Pc self-quenching at a minimum.[14] The QD concentrations, extinction coefficients, and diameters of the QDs were calculated by using Peng's method.[18]

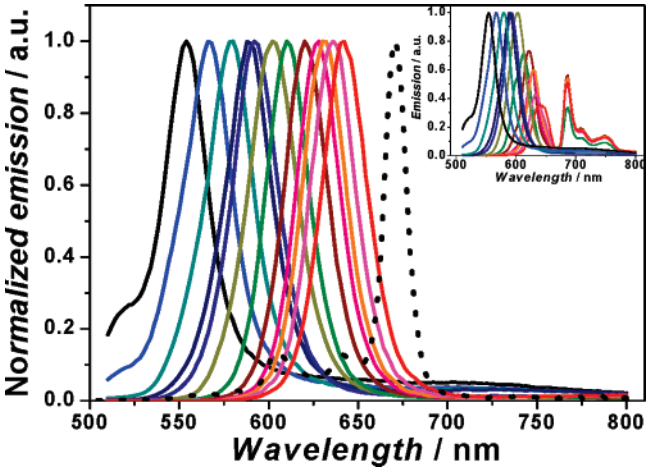

Figure 1. Normalized steady-state emission spectra of a series of CdSe QDs of different sizes; the black dotted line shows the corresponding absorption spectrum of the Pc. The inset shows the steady-state emission spectra of QD−Pc conjugates obtained using 500 nm as the excitation wavelength. The emission at 673 nm corresponds to the Pc excitation resulting from ET from the QDs.

Instrumentation. The synthesized QDs and conjugates were studied by steady-state absorption (Varian Cary 50) and fluorescence (Varian Eclipse fluorescence spectrophotometer) spectroscopy. For the study of the energy transfer dynamics, pure QDs and QD conjugates were investigated using femtosecond (fs) time-resolved laser spectroscopy following the 24 h conjugation period.[14] All samples were excited at 500 nm where the Pc does not absorb, in order to eliminate the interference due to direct excitation of the acceptor molecule. Broadband fs-laser pulses were used to probe the dynamics at the femtosecond time scale.[19] For fs measurements 2 mm cuvettes were used. All experiments were carried out at room temperature. Absorption spectra were collected before and after the time-resolved measurements and during the course of the experiment. No changes in the absorption spectra were observed.

Results and Discussion

Spectral Overlap Dependence. Based on previous studies,[14] it is known that van der Waals type interactions between TOPO-capped CdSe QDs and phthalocyanine molecules contribute to the binding of the energy acceptor to the QD surface. On the other hand, Pc molecules with amino or thiol functionality show a stronger interaction compared to alkyl terminated Pc's which do not show any ET efficiency. This observation indicates a Lewis acid−base interaction at the QD surface, similar to the established interaction between HDA (hexadecylamine) and CdSe QDs.

Figure 1 shows the normalized emission spectra of CdSe QDs along with the absorption spectrum of Pc 4. The Pc does not show any absorption at 500 nm and therefore allows for the exclusive excitation of the donor, and a clean photoinduced energy transfer from D to A is monitored. On varying the size of the QDs from 2.6 to 5.3 nm the respective emission maxima cover a wavelength range from 554 to 642 nm and show therefore a significant change in the overlap integral between QD emission and Pc absorption. The concentrations of the QDs were adjusted to have the same optical density at an excitation wavelength of 500 nm.

The steady-state emission spectra of CdSe−Pc conjugates are shown in the inset of Figure 1. As evident from the figure, the

(15) Peng. Z. A.; Peng, X. G. *J. Am. Chem. Soc.* **2001**, *123*, 183.
(16) Oleinick, N. L.; Antunez, A. R.; Clay, M. E.; Rihter, B. D.; Kenney, M. E. *Photochem. Photobiol.* **1993**, *57*, 242.
(17) Dayal, S.; Krolicki, R.; Lou, Y.; Qiu, X.; Berlin, J. F.; Kenney, M. E.; Burda, C. *Appl. Phys. B* **2006**, *84*, 309.
(18) Yu, W. W.; Qu, L.; Guo, W.; Peng, X. *Chem. Mater.* **2003**, *15*, 2854.
(19) Lou, Y.; Chen, X.; Samia, A. C.; Burda, C. *J. Phys. Chem. B* **2003**, *107*, 12431.

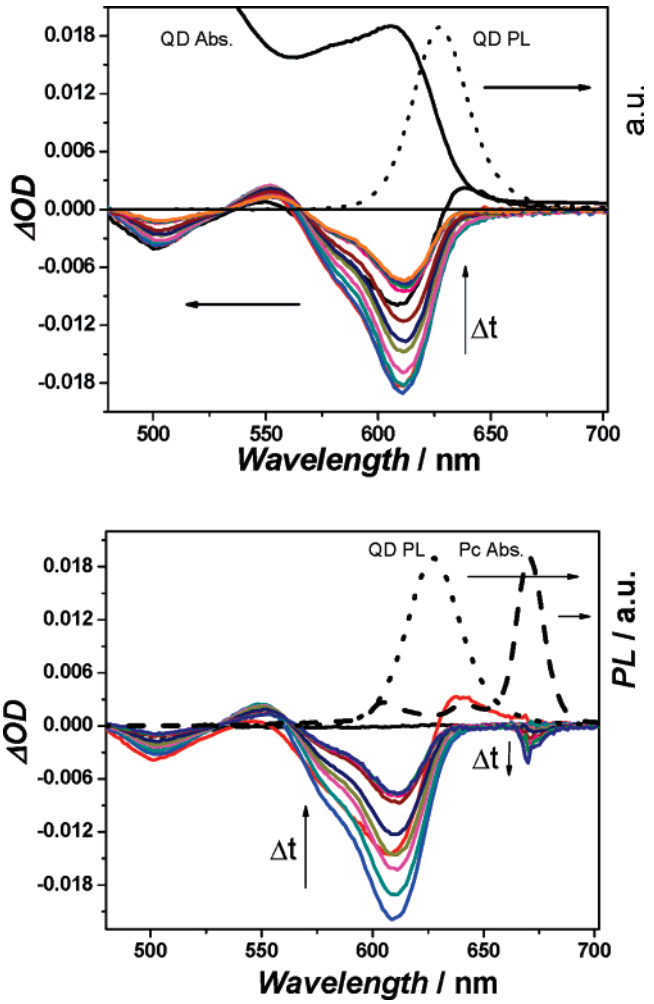

Figure 2. Femtosecond spectra of pure QDs (top) and QD−Pc conjugates (bottom). 500 nm wavelength light was used for the excitation of both the QDs and their conjugates. A bleach maximum assigned to ground state bleach of the QDs was observed at 610 nm. For the conjugates one additional bleach signal at 673 nm was observed. Steady-state absorption (solid) and emission spectra for QDs (dotted) and of Pc (dashed) are added in arbitrary units to the figure for comparison.

conjugation of the Pc to the QDs results in a quenching of the QD emission and the formation of a new emission peak at 673 nm corresponding to ET-induced Pc excitation. A strongly QD size-dependent quenching was observed.

The QD and QD conjugate samples were studied with time-resolved femtosecond spectroscopy with a resolution of 120 fs. The excitation pump power was adjusted to have an average of one photon per QD to minimize the effect of multiphoton absorption,[20,21] since an increase in number of absorbed photons per quantum dot is known to result in Auger recombinations.[22] Figure 2 shows the real-time transient absorption spectra of pure QDs and their conjugates with the Pc. A negative differential absorption band with an extremum at 610 nm could be assigned to the bleaching signal of the ground state QD absorption, and a positive transient absorption signal was observed at 640 nm, which decays in the first few picoseconds as commonly observed for QDs. However, in addition one finds for the conjugates that

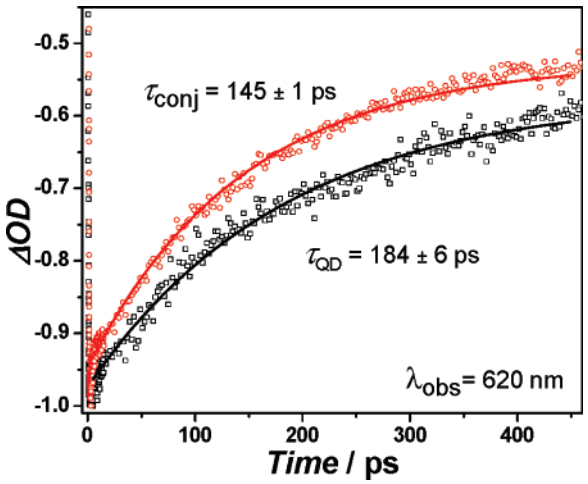

Figure 3. Typical normalized time-resolved kinetic traces for QDs (black squares) and conjugates observed at 620 nm (red circles) and the corresponding monoexponential fits (solid lines). Shown are the kinetic traces for 5.2 nm QDs with emission maxima at 635 nm.

the QD bleach signal decays faster and a negative transient signal appears consecutively at 673 nm, which could be assigned to the ground state bleach of the Pc. The transient bleaching of the Pc is due to the indirect excitation due to the ET.

The relaxation dynamics of the photoexcited CdSe QDs and their conjugates were monitored at the respective QD bleach wavelengths, and kinetic traces are shown in Figure 3. A faster decay for the QD bleach was observed in the presence of the energy acceptor, due to the availability of additional energy relaxation pathways.

The steady-state energy transfer efficiency $\phi_{ET}^{St.State}$ was calculated by using eq 1.

$$\phi_{ET}^{St.State} = 1 - I_{DA}/I_D \qquad (1)$$

where, I_D and I_{DA} are the relative integrated intensities of the donor emission in the absence and presence of the acceptor. The transfer efficiency ϕ_{ET}^{Kin}, based on the lifetimes, was calculated from the lifetime measurements of the donor, in the absence (τ_D) and presence (τ_{DA}) of the acceptor by using eq 2.

$$\phi_{ET}^{Kin} = 1 - \tau_{DA}/\tau_D \qquad (2)$$

The overlap integral was calculated from the emission spectra of CdSe QDs and absorption spectra of Pc 4 according to Lakowicz.[23]

$$J = \int f_D(\lambda)\epsilon_A(\lambda)\lambda^4 \, d\lambda \qquad (3)$$

where J is the overlap integral (M^{-1} cm^{-1} nm^4), $f_D(\lambda)$ is the normalized emission spectrum of the donor, $\epsilon_A(\lambda)$ is the absorption coefficient of the acceptor at wavelength λ and is expressed in M^{-1} cm^{-1}, and λ is used in nanometers.

The decay constants τ_D and τ_{DA} obtained from lifetime measurements are related to the ET rate constant (k_{ET}), fluorescence emission rate constant (k_{fl}) and the rate constants for all nonradiative relaxation processes (k_{nr}) as given in eq 4.

$$\tau_{DA}^{-1} = k_{ET} + k_{fl} + k_{nr} \qquad \tau_D^{-1} = k_{fl} + k_{nr} \qquad (4)$$

(20) Klimov, V. I.; McBranch, D. W. *Phys. Chem. B* **1997**, *55*, 13173.
(21) Burda, C.; Link, S.; Mohamed, M. B.; El-Sayed, M. *J. Chem. Phys.* **2002**, *116*, 3828.
(22) Klimov, V. I.; Mikhailovsky, A. A.; McBranch, D. W.; Leatherdale, C. A.; Bawendi, M. G. *Science* **2000**, *287*, 1011.
(23) Lakowicz, J. R. *Principles of fluorescence spectroscopy*, 2nd ed.; Kluwer Academic/Plenum Publishers: New York, 1999.

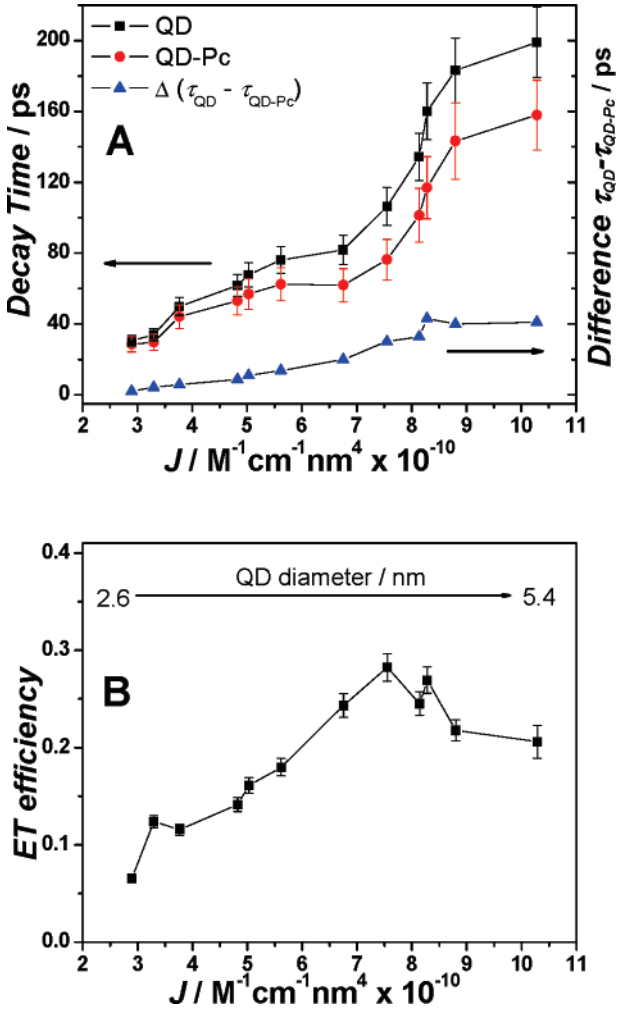

Figure 4. (A) Excited-state lifetimes of QDs and their DA conjugates as a function of the overlap integral. (B) Dependence of ET efficiency calculated according to eq 2 on the spectral overlap integral *J*.

The rate constant for the ET can therefore be determined by eq 5.

$$k_{ET} = \tau_{DA}^{-1} - \tau_{D}^{-1} \quad (5)$$

Rate constants in the range of $1.3 \times 10^9 - 4.2 \times 10^{10}$ s^{-1} were obtained.

The decay rates of the QD relaxation dynamics were obtained by fitting monoexponential functions to the measured kinetics and are plotted as a function of QD size in Figure 4A. A slower decay rate was observed for larger QDs. Based on previous work,[24,25] we infer that this is due to better surface passivation and less surface defects for larger QDs. Correspondingly, the conjugates follow a similar but not exactly the same trend in relaxation times as the pure QDs. The faster decay for conjugates of larger QDs can be explained by better spectral overlap of the QD emission with the Pc absorption. But, as seen in Figure 4B, the ET efficiency does not show a linear dependence on the overlap integral as predicted by Förster theory.

Comparing the conjugates in Figure 4B, there is a 3-fold increase in the overlap integral and the energy transfer efficiency

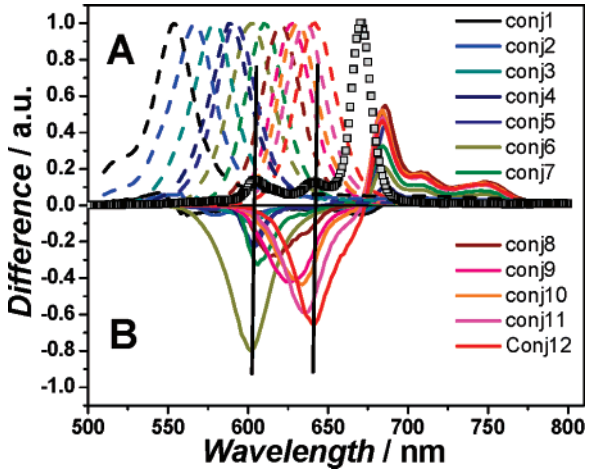

Figure 5. (A) Steady-state emission of pure QDs of 2.6−5.4 nm in diameter (dashed lines) and Pc 4 absorption (gray squares). (B) Difference spectra (solid lines) of DA conjugate emission minus pure QD emission showing increased emission at $\lambda > 670$ nm and emission quenching for $\lambda < 670$ nm. Both show maxima at 600 and 630 nm showing that the QD emission quenching is maximized where the acceptor absorbance peaks.

improves from 5% to 30%. However, the changes in efficiency are not monotonously increasing. There is an efficiency maximum for 5.0 nm QDs; for larger QDs the efficiency decreased again. This nonlinear dependence of transfer efficiency and transfer rate constant on spectral overlap indicates additional non-Förster-type components to the overall ET process. It is also evident that nonlinearities set in for small QDs. However, the two nonlinear regimes may possibly occur due to the same effect: involvement of surface states. The small QDs have a less favorable overlap integral to the Pc absorption. As the difference spectra in Figure 5 (the emission of QDs after conjugation minus the emission of QDs before conjugation of the same QD) show, the unexpected increase in ET efficiency is due to the strong involvement of surface states. The emission quenching occurs for the larger QDs with good spectral overlap mainly from the band edge states, while, for small QDs with negligible overlap, additional involvement of mid-band gap states in the ET process occurs. As shown in Figure 5B, the smallest QDs show quenching features which are significantly red-shifted from their band gap energy so that with the involvement of band gap states a spectral overlap is realized. Based on this we find that a surface-mediated ET can take place when band edge emission does not lead to efficient overlap. This produces a resonance between D and A that is not possible based on purely intrinsic electronic states and leads to the nonlinear efficiency curve for small QDs. For the largest QDs > 5 nm, intrinsic band edge states are in resonance with the acceptor absorbance and there is less coupling with the surface states visible, which would be red-shifted beyond 670 nm. This leads to the lesser ET efficiency measured for the larger QDs.

Surface Alteration. We further studied the ET efficiency and dynamics in core−shell CdSe−ZnS QDs and compared them with the core CdSe QDs to better understand the involvement of QD surface states. Surface capping or passivation of QDs with an inorganic or organic capping layer influences the characteristic absorption properties very little. However, the impact of capping is tremendous on the emission quantum yield and excited-state dynamics of QDs due to elimination of surface

(24) Guyot-Sionnest, P.; Hines, M. A. *Appl. Phys. Lett.* **1998**, *72*, 686.
(25) Guyot-Sionnest, P.; Shim, M.; Matranga, C.; Hines, M. A. *Phys. Rev. B* **1990**, *60*, R2181.

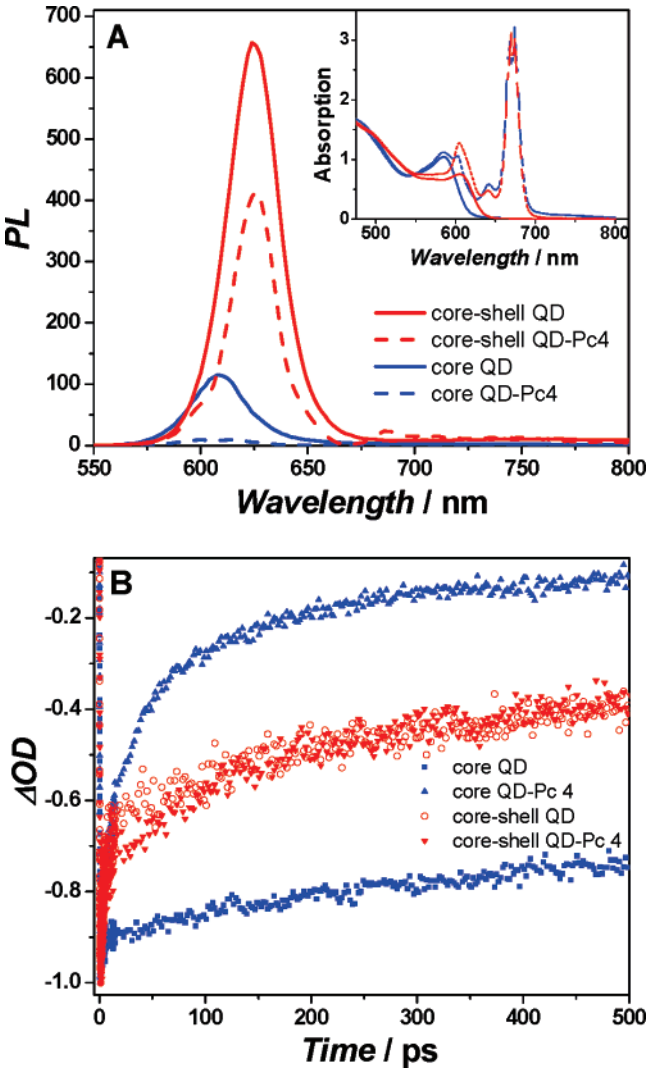

Figure 6. (A) Steady-state PL emission of QDs and their Pc conjugates. 500 nm excitation wavelength light was used for the excitation of the QDs. The inset shows the steady state absorption spectra of pure core and core−shell QDs and their conjugates with Pc 4. (B) Excited-state decay kinetics of pure core and core−shell QDs and their conjugates with Pc 4 shown up to 500 ps.

recombination sites.[26−28] For this study we synthesized the core and core−shell QDs emitting around 620 nm and conjugated them to Pc 4 molecules in the same fashion described above. Figure 6A shows the emission spectra of QDs and their conjugates. Respective absorption spectra are shown in the inset of Figure 6A.

With the same excitation conditions, the core−shell QDs exhibit much higher emission quantum efficiency. A peak around 673 nm was observed corresponding to the emission from the energy acceptor in the DA conjugates. We observed an ET efficiency of 40% for a core−shell QD emission compared to 80% ET efficiency in core CdSe QDs. Figure 6B shows the excited-state kinetics of QDs and their conjugates. Upon conjugation to acceptor molecules, significantly faster decay kinetics for unpassivated QDs were observed, while for ZnS-capped QDs no or very little accelerated decay was measured after conjugation to energy acceptor molecules.

Table 1. Steady State and Time-Resolved Energy Transfer Efficiencies for Core and Core−Shell QDs[a]

	steady-state ET efficiency	lifetime/ps	femtosecond ET efficiency
core QDs	-	244.5	-
core QDs−Pc	0.90	64.5	0.74
core−shell QDs	-	202.3	-
core−shell QDs−Pc	0.44	126.6	0.38

[a] The ET efficiencies calculated from steady state and time-resolved measurements are in good agreement. The ET from uncapped QDs was more efficient, presumably due to available surface states.

The faster decay dynamics upon addition of an acceptor molecule in the first case can be explained by the involvement of low-energy surface states involved in the energy transfer from the CdSe QDs to the energy acceptor. In ZnS-capped QDs these surface states are passivated by adding the inorganic capping layer of ZnS, and conjugation of a Pc did not result in enhanced quenching of the QD excited state. This observation further supports the model of involvement of surface states in the ET process and indicates the increased complexity when one involves quantum dots in processes such as ET. The excited-state decay lifetimes obtained by fitting the monoexponential decay curves are summarized in Table 1 along with steady-state and lifetime ET efficiencies.

Conclusion

In summary, we studied the effect of the surface states on the ET efficiency between CdSe QDs and phthalocyanine energy acceptors with steady-state and femtosecond time-resolved spectroscopy. We found that the QDs show a nonlinear dependence of the ET efficiency on spectral overlap due to intermediate surface states. On the other hand, QDs between 3.4 and 4.5 nm in diameter show a typical linear Förster dependence on the overlap integral. Furthermore, we observed a higher ET efficiency from uncapped core CdSe QDs compared to ZnS-capped core−shell CdSe QDs, which could again be explained by the involvement of QD surface states for the unpassivated QD. This study complements previous work, which reported components of capping-layer mediated ET between QDs and molecular energy acceptors.[14] Variability to tune the emission properties of QDs allows matching with many desirable energy acceptors for efficient energy transfer. This process can be surprisingly efficient, even when the spectral overlap of intrinsic electronic states is small, due to the mediation of QD surface states.

Acknowledgment. C.B. is grateful to BRTT funding from the State of Ohio. We thank Prof. Y. Lou for initial assistance on the femtosecond laser measurements and Prof. M. Kenney for providing high purity phthalocyanine compounds.

JA071457C

(26) Hines, M. A.; Guyot-Sionnest, P. *J. Phys. Chem. B* **1996**, *100*, 468.
(27) Dabbousi, B. O.; Rodriguez-Viejo, J.; Mikulec, F. V.; Heine, J. R.; Mattoussi, H.; Jensen, K. F.; Bawendi, M. G. *J. Phys. Chem. B* **1997**, *101*, 9463.
(28) Peng, X.; Schlamp, M. C.; Kadavanich, A. V.; Alivisatos, A. P. *J. Am. Chem. Soc.* **1997**, *119*, 7019.